2022

Experimental Investigation of a Micro-CHP Unit Driven by Natural Gas for Residential Buildings

Camila Davila

Nicolas Paulus

Vincent Lemort

Experimental Investigation of a Micro-CHP Unit Driven by Natural Gas for Residential Buildings

Camila DÁVILA[1]*, Nicolas PAULUS[1], Vincent LEMORT[1]

[1]University of Liège, Thermodynamics Laboratory,
Liège, Belgium

* Corresponding Author: cdavila@uliege.be

ABSTRACT

In this paper, an experimental performance analysis of a natural gas-driven micro-CHP unit is conducted. This system shows a global nominal heating output of 30.8 kW and is composed of a proton exchange membrane fuel cell (PEMFC), an integrated gas condensing boiler, and a storage tank. The PEMFC has a nominal thermal output of 1.1 kW and 750 W of electrical output. This unit is intended for residential applications to supply the related demands of space heating (SH) and domestic hot water (DHW) while producing electricity during operation.

Tests are carried out in the laboratory to characterize the behavior of the global system and its components under different demand requirements. To do so, an emulator of SH and DHW is installed and measures of gas consumption, heat production, and electricity consumption/generation are collected.

A test campaign based on the requirements of the EN 50465 is proposed and performed, where the base requirements are extended to a wider range of depart temperatures for SH and DHW; also, the effect of the imposed load over the system global performance is studied. After, both boiler and fuel cell are tested separately to characterize their contribution to the global system. The results show that the overall efficiency is mainly composed of the thermal output, being the electrical part a small fraction of the total, and with trends indicating that the lower the water outlet temperature, the higher the efficiency; the same trend is observed with respect to the heat demand since the lower this is, the higher the efficiency.

The results obtained for the boiler efficiency are close to those announced by the manufacturer, but for the fuel cell, the obtained results are varied due to the complexity of the system.

1. INTRODUCTION

Worldwide, ambitious goals and targets have been adopted by many countries to increase energy efficiency while decreasing greenhouse gas emissions within the 2030-2050 horizon.

One of the most significant sectors to provide one of the most significant contributions to climate mitigation by 2030 is the electricity sector, being a key area for the European Union to reach net climate neutrality by 2050. To reach this target, more policies and measures are needed to improve energy efficiency and encourage the deployment of renewable energy technologies (European Environment Agency, 2021).

On the other hand, the final energy consumption in the European Union fell by 8% between 2019 and 2020, results than are mostly linked to the measures adopted in response to the Covid-19 pandemic, with a significant effect on the transport sector. The energy consumption in households, however, remained stable, showing that a different approach must be followed to keep reducing the energy consumption and achieving the energy targets (European Environment Agency, 2022).

During the past years, the greenhouse gas emissions from electricity and heat used in buildings in Europe have been following a steady downward trend (European Environment Agency, 2021). If we look at the scenario per country, the actual percentage of change between 2005 and 2019 regarding greenhouse emissions from energy used in buildings has already overpassed the WEM (With Existing Measures) projections for 60% of the EU countries for the 2020-2030 period, while the other 40% need additional efforts to improve their performance for the same period (European Environment Agency, 2021).

Within this context, micro combined heat and power (CHP) systems appear as an interesting solution since they can provide electric power and hot water simultaneously based on a single energy source (usually natural gas or biogas), increasing fuel energy utilization and the system efficiency up to 20% by heat recovery and storage on an external water tank (Ou, Yuan, & Kim, 2021). The latter allows also to have better synchronization between the heat and electricity demands, which is usually a problem while using cogenerative systems (Barbieri, Melino, & Morini, 2012). Even more, if it is well-sized, the integration of micro CHP systems into the residential sector offers benefits such as reduction of primary energy use and minimization of the cost of electricity transmission and distribution losses since they are placed on-site. To that end, the electrical and thermal energy demand profiles must match the appliance's characteristics (De Paepe, D'Herdt, & Mertens, 2006) (Bianchi, Pascale, & Melino, 2013).

Within the available micro CHP technologies in the market, fuel cells are a promising technology for power and thermal generation due to their high efficiency, limited pollutants emissions, low noise levels, and reduced maintenance costs; systems based on such technologies can boost the energy efficiency in the residential sector and diminish the final energy consumption and pollutants produced as a consequence of the households energy needs (Cappa, Facci, & Ubertini, 2015).

2. DESCRIPTION OF THE SYSTEM

2.1 Proton exchange membrane fuel cell

The tested proton exchange membrane fuel cell (PEMFC) is a micro CHP unit designed for the production of space heating (SH), domestic hot water (DHW), and electricity for residential applications. Driven by natural gas, the system is divided into two main modules as shown in Figure 1.

The right-hand module is defined as the power generator module, composed of the fuel cell stack on the bottom and a gas condensing boiler on the top in order to meet the required peak heating demands. This module is connected to the natural gas supply pipeline, to a bidirectional power meter, and to the chimney to extract the combustion flue gases and allow the fresh air intake for both the boiler and the fuel cell stack. Both left and right side modules are connected on top by 4 depart and return pipes, generating two independent loops as shown in Figure 2. The heat generated as a by-product of the power generation process of the fuel cell stack is rejected by the water loop of the latter to a buffer tank on the cylinder module on the left side of Figure 1. This module is equipped with most of the hydraulics of the system and the 220-l buffer tank covers both DHW and SH demands. The technical features of the system are shown in Table 1.

Figure 1: Cylinder module (left) and Power Generator module (right) (Viessmann, 2018)

Table 1: PEMFC technical features

Heating output	TV/TR 60/40 °C 30.8 kW TV/TR 36/30 °C 0.9 kW
Electrical output FC*	0.75 kW
Thermal output FC*	1.1 kW
FC electrical efficiency	37% (H_i)
Overall FC efficiency	Up to 92% (H_i)
Peak load boiler thermal efficiency	Up to 98% (H_s)
Electric Power consumption	28 W standby 1400 W maximum
Gas consumption	3.38 m³/h natural gas
Permissible ambient temperature	Max.: 40°C Min.: 5°C

* *Output data: standard values to EN 50465 based on net calorific value*

2.2 Test bench

With the intention not to influence the performance of the machine, the sensors used to collect measurements inside the modules should not be invasive; this implies that, in terms of temperature measures, only surface thermocouples are installed on the pipes of the cylinder module and on the connections with the fuel cell module, represented by circles, in the disposition shown in Figure 2.

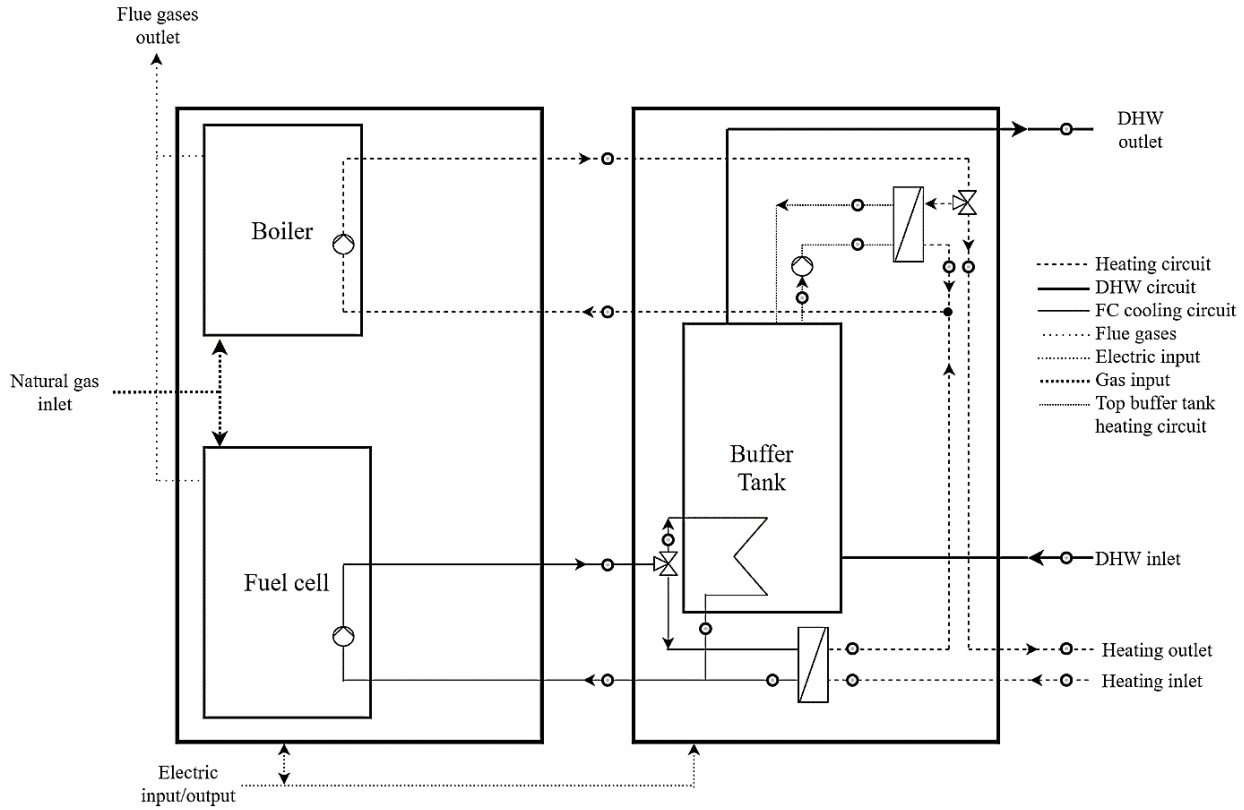

Figure 2: Location of surface thermocouples (grey circles) in the PEMFC modules

A rear-view scheme of the test bench is shown in Figure 3. The different sensors and their locations are given as well; the same symbology is used regarding thermocouples, with the difference that excluding the connecting tubes between both modules, thermocouples on immersion sleeves are used.

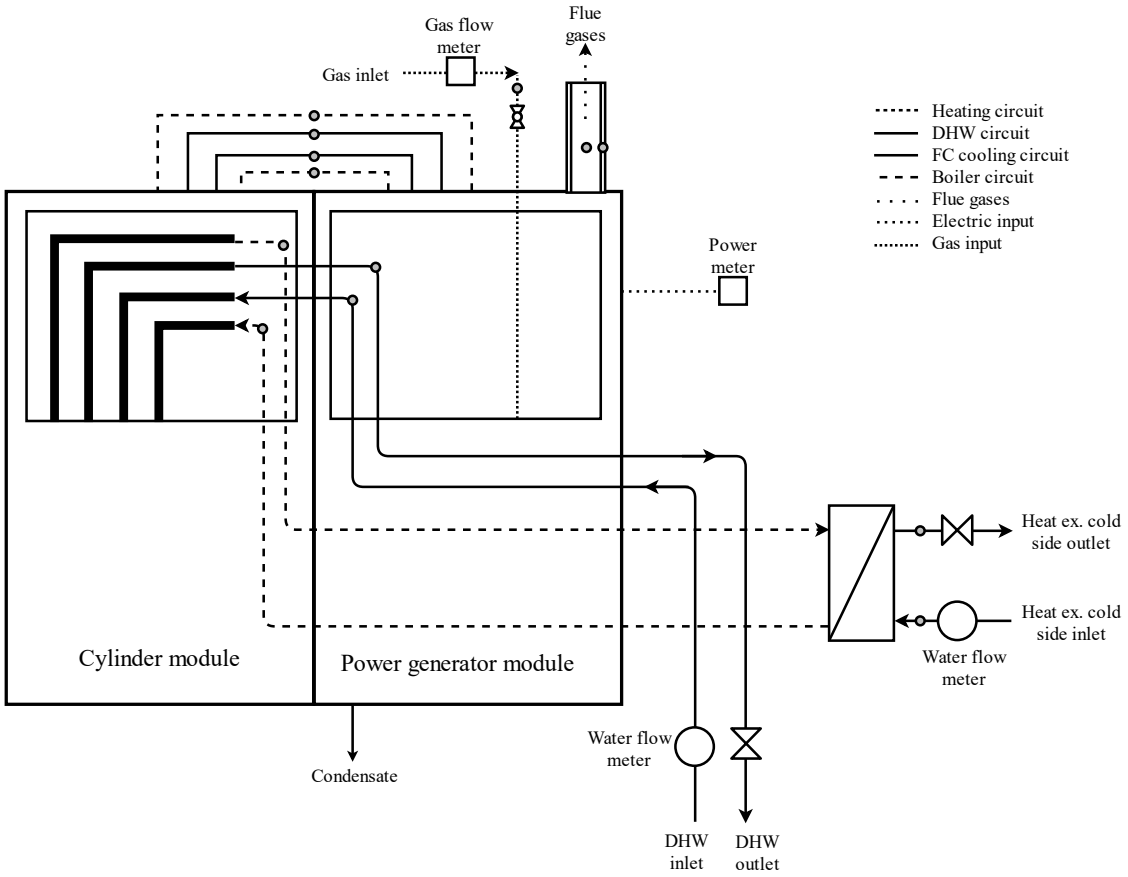

Figure 3: PEMFC test bench scheme rear-view

The cylinder module (heat sink) is placed next to the power generator module (heat source). The system is integrated to the rest of the test bench by 4 connections, including the supply and return flows intended for SH and DHW. The SH demand is emulated by a heat exchanger, the capacity of which is controlled by a valve that regulates the water flow rate on the cold side. In the same way, the demand of DHW is controlled by adjusting the opening of a valve at the outlet. Both the heat exchanger and the water pipes are insulated and close to the system to avoid heat losses. The measures of gas and electricity are realized on the supply lines of the system. The bidirectional electrical power meter shows both, the net electrical energy consumed and generated; the generated power exported to the grid is reduced by the power consumed by the operation of the PEMFC itself.

3. TESTING CONDITIONS

3.1 Test procedure

The heating process of the buffer tank is carried out by both the boiler and the fuel cell, and it always develops in the same way, ending when the buffer tank heats up to 50-52°C.

During the heating cycle, first, the boiler starts and heats the upper part of the buffer tank to the target temperature; this process is fast due to the large thermal power of the boiler (30.8 kW_{th}). In the meantime, the fuel cell enters on *Start Phase* before getting into *Power and heat generation Phase*; once this stage is reached, the fuel cell starts producing heat and electricity gradually until reaching its maximum thermal and electrical capacity of 1.1 kW_{th} and 0.75 kW_{el}, respectively. The heat produced by the fuel cell is rejected to the bottom part of the buffer tank and since its thermal capacity is small compared to the boiler, raising the temperature of this part of the buffer tank is a slow process.

If a heat demand is imposed on the system, the stored energy from the buffer tank is used from the top to the bottom following the temperature gradient generated by stratification; the temperature decrease will depend on the demand

water flow and how long the demand is maintained. If the demand stops, the tank will be heated; on the contrary, if heat is still requested, the system will be forced to deliver the produced heat immediately to the circuit that requires it. This second scenario is favorable to avoid the storage effect of the buffer tank on the performance estimation since the amount of energy stored is hard to quantify with the sensors used.

Having said that, the tests are forced to start once the buffer tank at its minimum temperature (around 17°C) and the behavior of the appliance (i.e., fuel cell and boiler) is steady. This steady-state varies from one test to another and depends on factors such as the flow demand (high or low) and the defined setpoint temperatures (DHW or SH).

3.2 Test matrix

In order to achieve the characterization of the system performance, the test campaign is based on the European Standard EN 50465. In terms of DHW, a step of 5 K is proposed until a minimum of (30 ± 2) K for delivery temperature; for SH, a step of 10 K is proposed with a minimum ΔT° of (20 ± 1) K between the depart and return flows. In terms of load, two different water flow rates are imposed (low and high) with the aim of visualizing their effect on efficiency. In terms of mode, tests are carried out with the option activated of DHW or SH production separately. The performed test campaign is shown in Table 2.

Table 2: PEMFC performed test campaign

DHW		
60 ± 2 °C	Low flow demand (Valve 50%)	High flow demand (Valve 100%)
55 ± 2 °C		
50 ± 2 °C		
45 ± 2 °C		
40 ± 2 °C		
35 ± 2 °C		
30 ± 2 °C		

SH		
Δ(20 ± 1) K	Low flow demand (Valve 50%)	High flow demand (Valve 100%)
Δ(30 ± 1) K		
Δ(40 ± 1) K		
Δ(50 ± 1) K		
Δ(60 ± 1) K		

These results give a first impression of the performance of the system, but they are not conclusive to perform a complete description of the appliance. To do so, it is important to characterize each component, fuel cell and boiler, separately.

Through the control panel display of the appliance, it is possible to turn off the fuel cell and work just with the boiler; then, the characterization of the boiler is done this way. Unfortunately, it is not possible to turn off the boiler and use exclusively the fuel cell heat and electrical power, so in an attempt to characterize the fuel cell stack, an alternative to bypass the control of the system and perform tests just with the fuel cell is proposed. This consists in disconnecting the ignition wire of the boiler to cause a failure and disable the operation of the latter. By doing so, the whole production and consumption of the system depend on the fuel cell only.

As shown in Figure 2, the fuel cell stack rejects the heat to the buffer tank by means of a heat exchanger. The water flow rate of this loop is unknown but is estimated to be very small due to the nominal thermal output of the fuel cell; therefore, since it is not possible to estimate directly the fuel cell efficiency, a different method is applied.

The previous tests were conceived to avoid the effect of the storage of the buffer tank; now, the thermal and electrical efficiencies of the fuel cell are estimated based on the heat released to the buffer and the time required to increase its temperature from an initial to a final state top and bottom temperatures of the buffer tank. This, however, adds a new challenge since the available information does not allow us to know *a priori* where the temperatures are being measured, i.e., where the thermocline is located as exemplified in Figure 4.

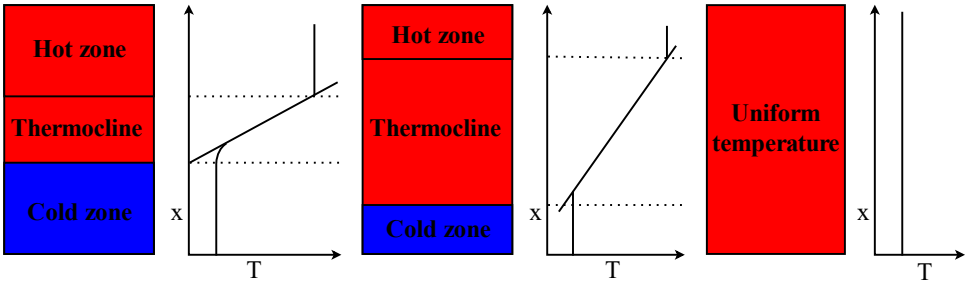

Figure 4: Graphical representation of the thermocline in the buffer tank

Daily tests divided into morning and evening are proposed based on different adaptations of load profiles recommended by the official journal of the European Union as shown in Table 3. These profiles differ in the requested water flow and the duration of the demand imposed, following a daily cycle as shown in Figure 5.

Table 3: Daily tests profiles description to estimate the fuel cell efficiency, morning and evening sessions

	Profile		
	A	**B**	**C**
Morning	1 shower 10 minutes 6 l/min	2 showers 20 minutes 10 l/min	1 shower 10 minutes 8 l/min
Evening	2 showers 30 minutes 6 l/min	3 showers 60 minutes 10 l/min	2 showers 20 minutes 8 l/min

The tests start in the morning with a homogeneous hot buffer tank. Then, a demand is imposed for the mentioned duration depending on the selected profile (see Table 3), cooling down the buffer till a certain level. This triggers the fuel cell module that starts heating the buffer till the beginning of the evening session when the second load is imposed. Once this session is ended, the fuel cell module heats up the buffer till the next day, arriving at the same initial point and closing the cycle.

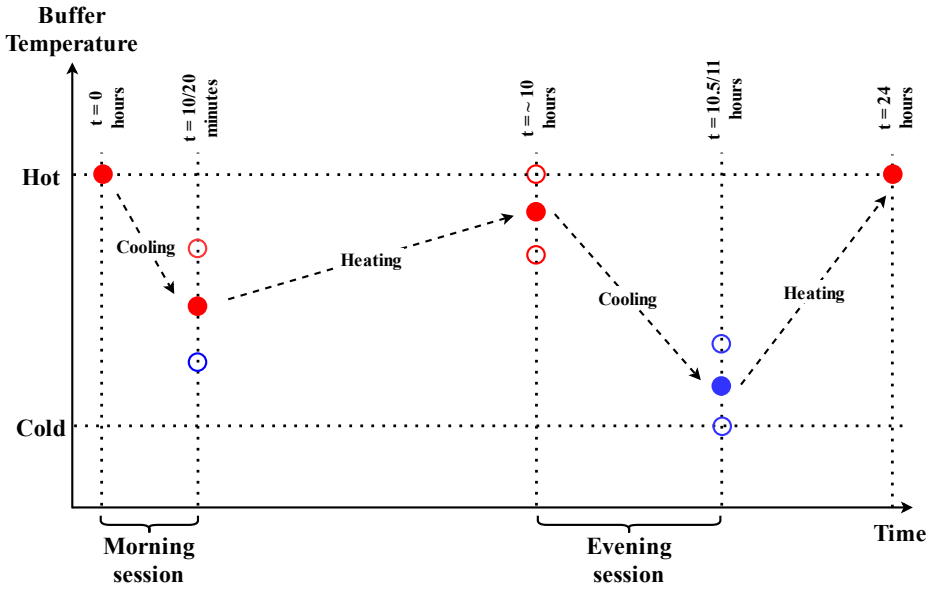

Figure 5: Daily tests 24 hours cycle evolution for fuel cell-only performance estimation

4. RESULTS

Data related to the appliance's consumption of natural gas, water flow, and temperatures associated with each test performed are collected and shown in Table 4. For every test the electricity production was 0.75 kW. The laboratory indoor conditions were between 20-25 °C and atmospheric pressure (1 bar). The steady-state data collecting period was 45 minutes per test.

Table 4: Experimental data collected

	DHW High flow demand (Valve 100%)				DHW Low flow demand (Valve 50%)			
	Gas Consumption [m3]	Water Consumption [m3]	Mean ΔT [K]	Test duration [s]	Gas Consumption [m3]	Water Consumption [m3]	Mean ΔT [K]	Tests duration [s]
60±2°C	2.353	0.809	22.913	2718	2.001	0.414	38.253	2728
55±2°C	2.399	0.827	23.173	2772	1.924	0.420	36.459	2739
50±2°C	2.249	0.801	22.476	2682	1.612	0.394	32.680	2627
45±2°C	1.936	0.809	19.316	2713	1.536	0.434	28.088	2834
40±2°C	1.593	0.808	16.013	2705	1.207	0.412	23.909	2695
35±2°C	1.245	0.800	12.770	2688	0.959	0.415	19.281	2725
30±2°C	0.915	0.788	9.487	2653	0.754	0.414	14.727	2726
	SH High flow demand (Valve 100%)				SH Low flow demand (Valve 50%)			
	Gas Consumption [m3]	Water Consumption [m3]	Mean ΔT [K]	Test duration [s]	Gas Consumption [m3]	Water Consumption [m3]	Mean ΔT [K]	Test duration [s]
60±1°C	2.429	1.128	17.205	2693	2.386	0.662	29.204	2678
50±1°C	2.010	1.123	14.650	2696	2.001	0.668	24.432	2677
40±1°C	1.640	1.125	12.055	2676	1.653	0.675	20.066	2665
30±1°C	1.208	1.137	8.756	2711	1.192	0.678	14.433	2698
20±1°C	0.844	1.144	5.958	2705	0.828	0.680	9.809	2693

Test performed	DHW 100%	DHW 50%	SH 100%	SH 50%
HHV [kWh/Nm^3]	11.6003	11.5730	11.4588	11.3016

The global efficiency of the system for each test was estimated as is shown in equation (1); the thermal and electrical efficiencies of the system were estimated as shown in equation (2) and equation (3).

$$\boldsymbol{\eta}_{\text{syst}} = \frac{\dot{m} * cp * \Delta T + \dot{W}_{el}/1000}{\dot{V}_{gas} * HHV} \quad (1)$$

$$\boldsymbol{\eta}_{\text{th}} = \frac{\dot{m} * cp * \Delta T}{\dot{V}_{gas} * HHV} \quad (2)$$

$$\boldsymbol{\eta}_{\text{el}} = \frac{\dot{W}_{el}/1000}{\dot{V}_{gas} * HHV} \quad (3)$$

Using these equations, the results of electrical, thermal and global efficiencies can be computed for each test. The high and low water flow demands are 0.298 [kg/s] and 0.152 [kg/s] respectively. The results are shown in Table 5 and Table 6.

Table 5: Electrical, thermal and global efficiencies of the system for DHW tests

	High flow demand			**Low flow demand**		
	η_{syst}	η_{th}	η_{el}	η_{syst}	η_{th}	η_{el}
T2, DHW 60°C	0.807	0.790	0.018	0.821	0.796	0.024
T3, DHW 55°C	0.818	0.800	0.018	0.826	0.799	0.026
T4, DHW 50°C	0.821	0.802	0.019	0.834	0.803	0.030
T5, DHW 45°C	0.832	0.809	0.023	0.829	0.797	0.032
T6, DHW 40°C	0.841	0.814	0.028	0.860	0.820	0.041
T7, DHW 35°C	0.858	0.822	0.035	0.889	0.838	0.051
T8, DHW 30°C	0.867	0.819	0.048	0.877	0.812	0.065

Table 6: Electrical, thermal, and global efficiencies of the system for SH tests

	High flow demand			**Low flow demand**		
	η_{syst}	η_{th}	η_{el}	η_{syst}	η_{th}	η_{el}
T13, ΔT 60 K	0.831	0.811	0.020	0.855	0.834	0.021
T12, ΔT 50 K	0.855	0.831	0.025	0.864	0.839	0.025
T11, ΔT 40 K	0.869	0.839	0.030	0.874	0.843	0.030
T10, ΔT 30 K	0.877	0.836	0.041	0.887	0.845	0.042
T9, ΔT 20 K	0.878	0.820	0.058	0.889	0.829	0.060

The results for the boiler efficiency are given in Table 7. In this case, the hydraulic connections shown in Figure 2 allow a direct efficiency estimation using equations (1) and (2), where the system is now considered only as the boiler and the electrical consumption penalizes the efficiency of the system.

Table 7: Boiler efficiency results obtained during boiler-only operation

Profile		**A**	**B**	**C**
Morning	Thermal energy out. [kWh]	3.227	9.219	4.176
	Gas energy cons. [kWh]	3.614	10.510	4.321
	Electrical energy cons. [kWh]	0.019	0.047	0.024
	η_{th}	0.893	0.877	0.966
	η_{syst}	0.888	0.873	0.961
Evening	Thermal energy out. [kWh]	9.620	28.179	8.430
	Gas energy cons. [kWh]	11.837	34.618	10.492
	Electrical energy cons. [kWh]	0.065	0.140	0.047
	η_{th}	0.813	0.814	0.804
	η_{syst}	0.808	0.811	0.800

The tests to estimate the fuel cell efficiency are performed several times each to minimize the error associated with the temperature measurement uncertainty in the buffer tank. To estimate the thermal efficiency just the heating periods are considered where it is assumed that half of the buffer tank is at T° top and half at T° bottom, leading to the definition of a ΔT° top and ΔT° bottom evaluated between the initial and final time of a heating period as shown in Figure 6; that is to say, i.e., that for the morning heating period an initial and final top and bottom temperatures are considered for the buffer tank, giving rise to a morning ΔT° top and a morning ΔT° bottom. This principle is applied as shown in equation (4) for a daily estimation and the results are summarized in Table 8.

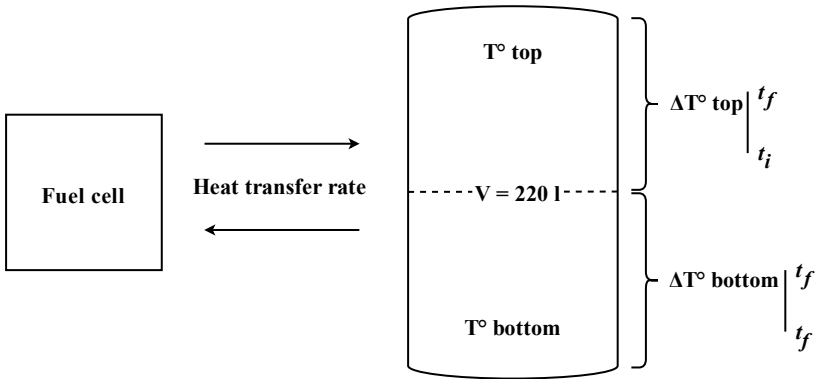

Figure 6: Buffer tank temperatures definition for fuel cell efficiency estimation

$$\eta_{\text{th, fc}} = \frac{0.5 * V_w * \rho_w * cp_w * (\Delta T_{top,m} + \Delta T_{bottom,m} + \Delta T_{top,e} + \Delta T_{bottom,e})}{3600000 * V_{gas} * HHV} \quad (4)$$

Table 8: Fuel cell efficiency estimation results

Profile		**A**	**B**	**B**	**C**	**C**	**C**
Start Morning	T° top	55	58	54	59	59	58
	T° bottom	55	58	54	59	59	58
End Morning	T° top	55	23	21	58	58	57
	T° bottom	49	20	20	44	48	44
Start Evening	T° top	58	51	50	57	50	57
	T° bottom	58	51	50	57	50	57
End Evening	T° top	25	18	19	27	24	27
	T° bottom	21	18	18	21	21	22
	Th. Power[kW]	0.442	0.690	0.722	0.439	0.344	0.441
	Electrical eff.	0.301	0.319	0.295	0.295	0.328	0.292
	Thermal eff.	0.179	0.308	0.290	0.175	0.152	0.173
	Global eff.	0.480	0.626	0.585	0.470	0.480	0.465

5. CONCLUSIONS AND PERSPECTIVES

In this work, the characterization of a natural gas-driven micro-CHP unit has been performed. The heating output of the system is based on a proton exchange membrane fuel cell (PEMFC) and a gas condensing boiler. Tests were carried out in a laboratory environment to characterize the behavior of the global system and its components, both boiler and fuel cell, separately, to study their contribution to the global system performance under different requirements.

The results obtained for the overall efficiency of the system in steady-state avoiding the thermal buffer effect show that it is mainly composed of the thermal output, the electrical part being a small fraction of the total. A maximum value of 0.889 for the global efficiency of the system was reached, where the electrical contribution does not exceed 6% of the total. The trends indicate that the lower the water outlet temperature, the higher the efficiency as expected. To a lesser extent, the lower the demand, the higher the efficiency.

The results obtained for the boiler efficiency are between those announced by the manufacturer, reaching 0.961 as the maximum value in the laboratory. For the fuel cell, the results are varied due to the complexity of the system. The thermocline inside the buffer and the lack of information regarding the cooling fluid mass flow rate and its temperatures lead to a maximum global efficiency value of 0.626 obtained with the proposed method, where 0.319 corresponds to the electrical contribution and 0.38 to the thermal contribution. However, having 30% as the maximum obtained value for thermal efficiency is unexpectedly low, especially if the global efficiency for this case is 62% and far from the 92% announced.

It is possible to assure that the results are far from the performance indicated in the datasheet, especially in relation to the thermal efficiency of the fuel cell. The latter is mainly due to the lack of information regarding the water flow in the cooling circuit of the fuel cell loop, reason why more tests must be done to improve the accuracy of the results with the proposed method or an alternative must be sought.

NOMENCLATURE

cp	Specific heat capacity	(kJ/kg-K)
HHV	Normalized high heating value	(kWh/Nm^3)
$\dot{m}$	Masic flow	(kg/s)
T	Temperature	(K)
V	Volume	(m^3)
$\dot{V}$	Volumetric flow	(m^3/s)
$\dot{W}$	Electrical power	(kW)

Subscript

e	Evening
el	Electric
f	Final
fc	Fuel cell
gas	Gas
i	Initial
m	Morning
$syst$	System
th	Thermal
w	Water

Greek symbols

Δ	Difference
η	Efficiency
ρ	Density

REFERENCES

Barbieri, E. S., Melino, F., & Morini, M. (2012). Influence of the thermal energy storage on the profitability of micro-CHP systems for residential building applications. *Applied Energy, 97*, 714-722.

Bianchi, M., Pascale, A. D., & Melino, F. (2013). Performance analysis of an integrated CHP system with thermal and Electric Energy Storage for residential application. *Applied Energy, 112*, 928-938.

Cappa, F., Facci, A. L., & Ubertini, S. (2015). Proton exchange membrane fuel cell for cooperating households: A convenient combined heat and power solution for residential applications. *Energy, 90*, 1229-1238.

De Paepe, M. D., D'Herdt, P., & Mertens, D. (2006). Micro-CHP systems for residential applications. *Energy Conversion and Management, 47*, 3435-3446.

European Environment Agency. (2021). *Greenhouse gas emission intensity of electricity generation by country.*

European Environment Agency. (2021). *Greenhouse gas emissions from energy use in buildings by country.*

European Environment Agency. (2021). *Greenhouse gas emissions from energy use in buildings in Europe.*

European Environment Agency. (2022). *Primary and final energy consumption in the European Union.*

Ou, K., Yuan, W.-W., & Kim, Y.-B. (2021). Development of optimal energy management for a residential fuel cell hybrid power system with heat recovery. *Energy, 219*, 119499.

Viessmann. (2018). *Power-generating heating system.*

ACKNOWLEDGMENT

The authors thank Gas.be for the financial support to this research project.